



On forecasting wet-snow avalanche activity using simulated snow cover data



Sascha Bellaire^{a,b,*}, Alec van Herwijnen^a, Christoph Mitterer^{c,d}, Jürg Schweizer^a

^a WSL Institute for Snow and Avalanche Research SLF, Davos, Switzerland

^b Institute of Atmospheric and Cryospheric Sciences, University Innsbruck, Austria

^c Avalanche Warning Service Tyrol, Austria

^d Institute for Infrastructure, Unit for Geotechnical and Tunnel Engineering, University of Innsbruck, Austria

ARTICLE INFO

Keywords:

Avalanche forecasting

Wet-snow avalanche

Snow cover modelling

Numerical weather prediction

ABSTRACT

Wet-snow avalanches are relatively poorly understood and difficult to forecast. By definition, water is required in the snow cover, thus assessing the liquid water content of the snow cover is of paramount importance for wet-snow avalanche forecasting. While evaluating wet-snow instability through field measurements is difficult, physically based snow cover models can be used to estimate the amount of liquid water within the snow cover using meteorological input. Recently, an index based on the liquid water content of the snow cover was suggested showing high potential to predict the onset of wet-snow avalanche activity. However, as the snow cover model was forced with data from automated weather stations (AWS) only a now-cast was possible. As snow cover conditions quickly change during snow melt, a forecast would be useful. For this study, we therefore force the 1-D physically based snow cover model SNOWPACK with data from the high-resolution numerical weather prediction model COSMO and investigate whether forecasting regional patterns of the onset of wet-snow avalanche activity is feasible. To validate the index, we compared simulations performed at the location of numerous AWS in the Swiss Alps with wet-snow avalanche observations from the corresponding region. Only by forcing SNOWPACK with data from automated weather stations up to the actual day and then adding the forecasted input data to produce a forecast led to results comparable to the simulations with station data only. While using this setup, the index was able to predict the onset of wet-snow avalanching with a probability of detection of > 80% for three winters between 2013 and 2016 and for two different climate regions in Switzerland. However, the false alarm ratio was high (up to 80%), suggesting that further refinements of the classification method are needed.

1. Introduction

Wet-snow avalanches release when melt water or rain infiltrates the snow cover and consequently weakens the snowpack. As water infiltration is a strongly non-linear process and the presence of water changes the snow properties, critical conditions for release are difficult to assess and often only prevail for a short period of time (e.g., Schneebeli, 2004; Trautman et al., 2006). Therefore, predicting wet-snow instability represents a great challenge for most operational avalanche forecasting services (Techel and Pielmeier, 2009).

Given the rather poor understanding of the formation process, statistical rather than physical models have been developed for wet-snow instability prediction (e.g., Baggi and Schweizer, 2009; Peitzsch et al., 2012; Romig et al., 2005). These studies showed that air temperature is a poor predictor and that the state of the snow cover is also a relevant

variable. Instead of considering air temperature, Mitterer and Schweizer (2013) suggested to assess melt water production based on the snow surface energy balance, which they modelled for virtual slopes of north- and south-facing aspect using the 1-D snow cover model SNOWPACK (e.g., Lehning et al., 1999). Hence, they considered drivers for melt water production, but not infiltration.

More recently, Mitterer et al. (2013) suggested an index for the onset of wet-snow avalanching (LWC_{index}). The index is based on the average liquid water content of the entire snow cover simulated with SNOWPACK. They suggested that the onset of wet-snow avalanching starts when an average volumetric liquid water content ($\theta_{w,v}$) of 3% is reached. Alternatively, Wever et al. (2016a) investigated whether ponding of water at capillary barriers was indicative of wet-snow avalanche occurrence. They forced SNOWPACK with data from automated weather stations located in the Alps, Central Andes and

* Corresponding author.

E-mail address: sascha.bellaire@gmail.com (S. Bellaire).

Pyrenees. They found a liquid water content of 5–6% locally within the snow cover to be a better predictor for wet-snow avalanche activity compared to other methods like the daily mean air temperature or the daily sum of the positive energy balance. In addition, the location or depth within the snow cover where the liquid water content was highest was found to be related to the size of wet-snow avalanches.

Mitterer et al. (2016) compared simulated snow stratigraphy, mean liquid water content and water infiltration within the snow cover to measurements with an upward-looking ground penetrating radar located in an avalanche slope (upGPR; Schmid et al., 2014). Measurement and simulations agreed fairly well and showed that increased wet-snow avalanche activity in the vicinity of the radar started when the mean volumetric liquid water content of the snow cover reached 1% and a significant diurnal increase in $\theta_{w,v}$ was observed. In three out of four melt seasons, the first arrival of water at the bottom of the snow cover coincided with the onset of wet-snow avalanche activity. These previous studies suggest that the index based on $\theta_{w,v}$ can be used to predict wet-snow avalanche activity. However, in these studies SNOWPACK was forced with weather station data, hence only a now-cast was possible. Moreover, it is not fully clear which threshold value of the liquid water content index is most appropriate for a given study site.

A different approach to wet-snow avalanche prediction was used by Helbig et al. (2015). They used numerical weather prediction (NWP) data to calculate wet-snow probability maps for the entire Swiss Alps based on a probability density function derived from detailed avalanche occurrence data. While their model performed reasonably well, they only used two meteorological parameters and noted that including snow cover information would likely improve the model performance. However, current manual snow cover observations do not provide the necessary spatial and temporal coverage, thus integrating snow cover models to simulate snow stratigraphy is required.

The two most advanced snow cover models are the French model CROCUS (Brun, 1989; Brun et al., 1992), which is used within the SAFRAN–SURFEX/ISBA/Crocus–MEPRA model chain (Durand et al., 1999; Lafaysse et al., 2013; Vionnet et al., 2012), and the Swiss snow cover model SNOWPACK (Bartelt and Lehning, 2002; Lehning et al., 2002a; Lehning et al., 2002b). Both models were already successfully driven with numerical weather prediction model data allowing to forecast the evolution of the snow cover (Bellaire and Jamieson, 2013a; Quéno et al., 2016; Vernay et al., 2015; Vionnet et al., 2016). So far, validation of such model chains mainly focused on snow height and stratigraphy (e.g., Bellaire and Jamieson, 2013a; Bellaire et al., 2011; Schirmer and Jamieson, 2015; Vionnet et al., 2012) and rarely on stability (e.g., Bellaire and Jamieson, 2013b; Vernay et al., 2015).

Therefore, we aim to force the snow cover model SNOWPACK with data from a NWP model to forecast changes in the liquid water content of the snow cover, as suggested by Mitterer et al. (2013), to predict the onset of wet-snow avalanche activity. We compare model output to wet-snow avalanche activity observed in two regions of the Swiss Alps for three winter seasons.

2. Data

2.1. Avalanche observations

Trained observers record avalanche occurrences on a daily basis within each forecasting region across Switzerland. We used observations from two regions (Fig. 1) Grisons (~7000 km²; Eastern Swiss Alps) and Valais (~5000 km²; Western Swiss Alps). Observers record avalanche occurrences along with corresponding characteristics including type of trigger (e.g. natural release or skier-triggered), size, aspect and elevation. In addition, observers estimate whether it was a dry- or wet-snow avalanche. For this study, we focus on wet-snow avalanches observed during three winter seasons between October 2013 and June 2016. During this period, a total of 352 wet-snow avalanches were recorded in the region of Valais and 751 in Grisons.

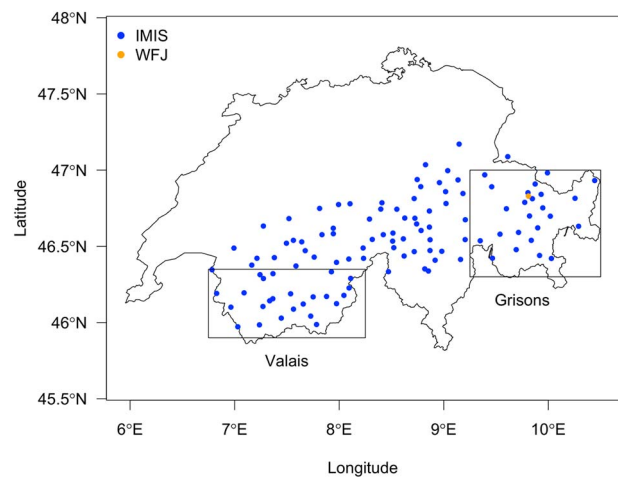


Fig. 1. Map of Switzerland showing the locations of the IMIS stations (blue, $N = 112$) as well as the location of the experimental site Weissfluhjoch (WFJ, orange). Rectangular show the two regions of Grisons and Valais. (For interpretation of the references to colour in this figure legend, the reader is referred to the web version of this article.)

These observations include all types of wet-snow avalanches, i.e. loose-snow avalanches, slab avalanches and possibly even some warm glide-snow avalanches, whether they released naturally or were triggered artificially. A distinction between these avalanche types was not possible, because the avalanche type was not consistently recorded. In addition, the avalanche type may be estimated from the debris, leading to an unknown degree of misclassification.

2.2. Meteorological data

To force the snow cover model SNOWPACK (see below), we used meteorological data from a network of automated weather stations (AWS) located between 1500 m and 3000 m a.s.l. across the Swiss Alps (Intercantonal Measurement and Information System: IMIS; Lehning et al., 1999). These IMIS stations were designed to provide meteorological and snow cover data for avalanche warning services; the locations were selected to be representative of the surrounding area. IMIS station data include air temperature (non-ventilated) and humidity, wind speed and direction, reflected short wave radiation, surface temperature as well as snow height.

To evaluate the accuracy of numerical weather prediction model data (see below), we used high quality meteorological data, namely air temperature (ventilated), incoming short wave radiation as well as incoming long wave radiation from a site located above Davos, Switzerland (Weissfluhjoch; 2540 m a.s.l.; Grisons, Eastern Swiss Alps, Fig. 1).

2.3. Numerical weather prediction (NWP) model data

When forecasting the snow cover conditions, we used data from the numerical weather prediction model COSMO to force the snow cover model SNOWPACK. COSMO is a non-hydrostatic limited-area model developed and maintained by the Consortium for Small scale Modelling (COSMO, www.cosmo-model.org). For our study, we used data from the operational version of COSMO operated by the Swiss Federal Office of Meteorology and Climatology (MeteoSwiss) with a horizontal resolution of 1.1 km (COSMO-1). This model (formerly 'LM', Doms and Schättler, 2002) is currently in operational use by different European weather forecasting services (Germany, Switzerland, Italy, Poland, Romania, Greece and Russia). The COSMO-1 domain extends about 1000 km in east-west direction and about 700 km in north-south direction with the Alps in its centre. COSMO-1 became fully operational in March 2016, is initiated 8 times a day with a lead-time of up to 33 h

(3 UTC run). Before March 2016, COSMO-1 was tested pre-operationally since October 2015. COSMO-1 data became available in August 2012, i.e. in principle data for the winter seasons between 2012 and 2016 are available. However, COSMO-1 was subjected to occasional changes in terms of model physics and domain extent especially until the summer of 2013. We therefore focus our analysis on the three winter seasons between October 2013 and June 2016. In the following, we will refer to COSMO-1 as COSMO.

3. Methods

3.1. Liquid water content index

Mitterer et al. (2013) defined a liquid water content index LWC_{index} as:

$$LWC_{index} = \frac{\overline{\theta_{w,v}}}{0.03} \quad (1)$$

where $\overline{\theta_{w,v}}$ is the mean volumetric liquid water content of the entire snow cover. A LWC_{index} of 1 indicates that water will likely percolate through the snow since at a liquid water content of 3% the transition from the pendular to the funicular regime starts (e.g. Denoth, 1980). Mitterer et al. (2016) suggested two critical thresholds for the onset of wet-snow avalanche activity depending on the scale of the study area and the flow regime, namely $LWC_{index} \geq 1$ and $LWC_{index} \geq 0.33$. The lower value proved to be useful when considering a single avalanche path.

3.2. SNOWPACK

We used the snow cover model SNOWPACK (Version 3.3.0, bucket mode for water transport scheme) to simulate snow stratigraphy for flat sites, i.e. the locations of the IMIS stations as well as for virtual south-facing slopes (38° incline, 180° azimuth). For the slope simulations incoming shortwave radiation was extrapolated according to Helbig et al. (2010).

In addition, the amount of liquid precipitation can be calculated by SNOWPACK. The model estimates the new snow density taking into account the current meteorological conditions (Schmucki et al., 2014) and calculates the liquid precipitation amount corresponding to the new snow depth. These estimated liquid precipitations amounts were compared to forecasted precipitation provided by COSMO (see below).

SNOWPACK can be forced with NWP data (COSMO) as well as IMIS data (IMIS). When using IMIS data, SNOWPACK was forced with reflected shortwave radiation, as well as snow surface temperature and measured snow height. This forcing of SNOWPACK using IMIS station data represents the most stable setup, which was validated in many studies (e.g. Lehning et al., 1999). These simulations therefore serve as the reference for this study.

To force SNOWPACK with NWP data we used COSMO forecasted data of the first 23 h after initiation at 00 UTC to create a daily time series with hourly time steps to then force the snow cover model SNOWPACK. Forcing data include COSMO forecasted incoming shortwave and incoming longwave radiation, precipitation, air temperature, relative humidity, wind speed and direction. COSMO data from the closest (Euclidian distance) grid-point to the corresponding IMIS stations were used. No corrections were made for the COSMO data except for correcting the air temperature using the elevation difference between the closest grid-point and the station using a wet-adiabatic lapse rate of 6.5 K km^{-1} .

3.3. Avalanche activity index (AAI)

To estimate the avalanche activity based on avalanche observations, we calculated the daily avalanche activity index (AAI) per region (Grisons and Valais) and for the elevation band between 2000 m and

2500 m a.s.l. as suggested by Schweizer et al. (2003). Wet-snow avalanche observations (i.e. all types) were weighted according to their size and summed up (Canadian avalanche size class; McClung and Schaerer, 2006); weights were 0.01, 0.1, 1, 10 and 100 for classes 1 to 5, respectively. As in Switzerland avalanche size is recorded by description rather than a categorical variable ranging from 1 to 5, we assigned avalanche sizes recorded as 'sluff' to 1, 'small' to 2, 'intermediate' to 3, 'large' to 4 and 'very large' to 5.

3.4. Forecast performance

To assess the performance of the COSMO forecast during the snow season we first compared historical daily COSMO runs performed at 00 UTC from MeteoSwiss to measured meteorological parameters relevant for the snow cover evolution. Forecasted data of air temperature, incoming shortwave radiation and incoming longwave radiation were compared to high quality data from a site located above Davos, Switzerland (Weissfluhjoch; 2540 m a.s.l.; Grisons, Eastern Swiss Alps, Fig.1).

Second, we compared the difference in snow height (hourly values) between SNOWPACK simulations forced with measured input data (IMIS) and the simulations forced with forecasted data (COSMO). We considered all IMIS stations and grouped them into three elevation bands, namely stations located below 2000 m a.s.l., between 2000 and 2500 m a.s.l. as well as stations above 2500 m a.s.l.

Third, we assessed whether the LWC_{index} was related to observed avalanche activity in the two regions. Regional avalanche activity was classified into non-avalanche days, defined as days with an AAI < 1, and avalanche days with an AAI ≥ 1 . For comparison, we used avalanche occurrence data from 1 January to 30 April between 2014 and 2016. The total number of days (N) was 361, i.e. 72 avalanche and 289 non-avalanche days for Grisons and 44 avalanche and 317 non-avalanche days for Valais. For each region, avalanche activity was then related to the median of the daily maximum value of the LWC_{index} considering all stations located in the corresponding region between 2000 m and 2500 m a.s.l., i.e. Grisons ($N = 16$) and Valais ($N = 14$).

To assess the performance of the LWC_{index} with regard to predicting the onset of wet-snow avalanche activity several performance measures were calculated with the definitions used in contingency tables (Table 1; e.g., Schweizer and Jamieson, 2007). Accordingly, the probability of detection (POD) is defined as (Wilks, 2011):

$$POD = \frac{d}{b + d} \quad (2)$$

the probability of non-events (PON):

$$PON = \frac{a}{a + c} \quad (3)$$

the false alarm ratio (FAR):

$$FAR = \frac{c}{c + d} \quad (4)$$

as well as the true skill statistic (TSS) defined as:

$$TSS = \frac{d}{b + d} - \frac{c}{a + c} \quad (5)$$

The probability of detection is also called sensitivity and the

Table 1
2 × 2 contingency table as used to calculate performance measures (compare Eqs. (2)–(5)).

		Observation	
		Stable	Unstable
Forecast	Stable	a: Correct stable	b: Misses
	Unstable	c: False alarms	d: Hits

probability of non-events is called specificity. A forecast should have a low false alarm ratio and predict stable and unstable conditions equally well, i.e. both the specificity and the sensitivity should be high.

Rather than using a fixed threshold value of the LWC_{index} to discriminate between avalanche days and non-avalanche days, such as 1 or 0.33 (Mitterer et al., 2016; Mitterer et al., 2013), we optimized the threshold value. We calculated the performance measures for various thresholds ranging from 0.01 to 1 with an increment of 0.01, whereas avalanche days were always defined as days with a maximum LWC_{index} value larger than the threshold. The performance for various thresholds can then be assessed in a receiver operating characteristics (ROC) graph, which illustrates the trade-off between hit rate and false alarm rate (e.g., Schweizer et al., 2009; Wilks, 2011). We selected the threshold with the highest true skill statistic as the optimal threshold.

4. Results

4.1. Meteorology and snow cover

4.1.1. Air temperature and radiation

Forecasted air temperature values from COSMO were generally lower than the measurements at Weissfluhjoch (Fig. 2a). The incoming shortwave radiation was generally overestimated and the incoming longwave radiation underestimated (Fig. 2b and c). The mean error (ME) and mean absolute error (MAE) for the period between October 2015 and June 2016 were $-2.0\text{ }^{\circ}\text{C}$ for the air temperature (MAE = $2.16\text{ }^{\circ}\text{C}$), 12.6 W m^{-2} for the incoming shortwave radiation (MAE = 34.4 W m^{-2}) and -22.0 W m^{-2} for the incoming longwave radiation (MAE = 28.0 W m^{-2}). A comparison (not shown) for the winter seasons between 2013 and 2015 showed very similar errors.

4.1.2. Precipitation

The total forecasted precipitation by COSMO for the winter season 2015–2016 was 973 mm compared to 1034 mm as calculated by SNOWPACK. Hence, the forecasted precipitation was within 6% of the estimated precipitation – in good agreement. However, on an hourly basis, the comparison between COSMO and SNOWPACK showed considerable scatter (Fig. 3a), which slightly improved when using daily sums (Fig. 3b). Comparing the cumulative density functions for daily precipitation suggests that smaller ($< 10\text{ mm}$) more frequent precipitation events were overestimated and larger events ($> 10\text{ mm}$) were underestimated (Fig. 3c).

4.1.3. Snow height

The differences in snow height (hourly values) between SNOWPACK simulations forced with measured input data (IMIS) and simulations forced with forecasted data (COSMO) are shown in Fig. 4 for three winter seasons (October to June) between 2013 and 2016. The snow height difference ($HS_{COSMO} - HS_{IMIS}$) was averaged over all stations located within one of three elevations bands, i.e. $< 2000\text{ m a.s.l.}$, between 2000 m a.s.l. and 2500 m a.s.l. , and $> 2500\text{ m a.s.l.}$ Until the end of March, the absolute difference in snow height was typically less than about 25 cm. Later in the season, a positive difference, i.e. too much snow simulated with COSMO, was found for stations above 2000 m a.s.l. and a negative difference for stations below 2000 m a.s.l. During the winter season 2015–2016, the snow heights provided by the COSMO simulations for stations below 2000 m were too low already as of mid-January.

4.1.4. Liquid water content index

Since the calculation of the LWC_{index} requires averaging the liquid water content over the entire snow cover, it is sensitive to the total snow height. Hence, an accurate simulation of the snow height is essential. Fig. 5 shows the mean difference between the LWC_{index} derived from simulations using COSMO data and IMIS data. Results are shown for the winter season 2015–2016 (February to May) for the three

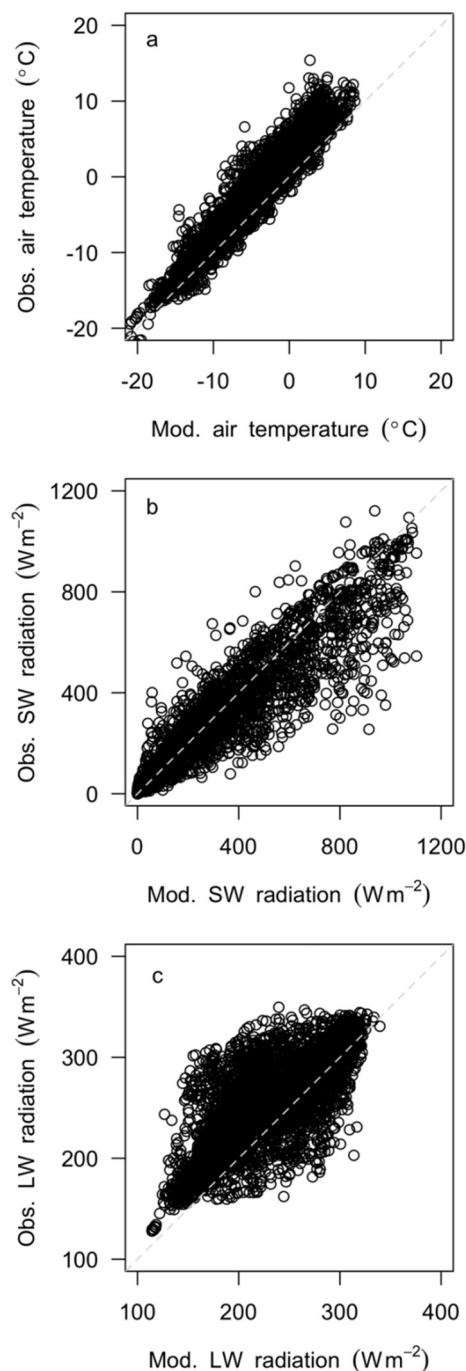


Fig. 2. Comparison of hourly forecasted (COSMO) and observed (Weissfluhjoch) meteorological key parameters for (a) air temperature, (b) incoming shortwave (SW) radiation, (c) incoming longwave (LW) radiation between October 2015 and June 2016. Dashed lines indicate the one-to-one relationship.

elevation bands. Simulations were carried out for a flat site, i.e. the location of the IMIS stations.

The LWC_{index} using COSMO data as input was in good agreement with the reference runs (IMIS) for stations above 2000 m a.s.l. between February and March (Fig. 5a), coinciding with the reasonable agreement of snow height in this period (Fig. 4b). The LWC_{index} for station below 2000 m a.s.l. was overestimated, which is also in line with the general underestimation of snow height for stations located in this elevation band. In April the LWC_{index} was underestimated for stations above 2500 m a.s.l. due to an overestimated snow height. For stations between 2000 and 2500 m a.s.l. , on the other hand, the LWC_{index} was

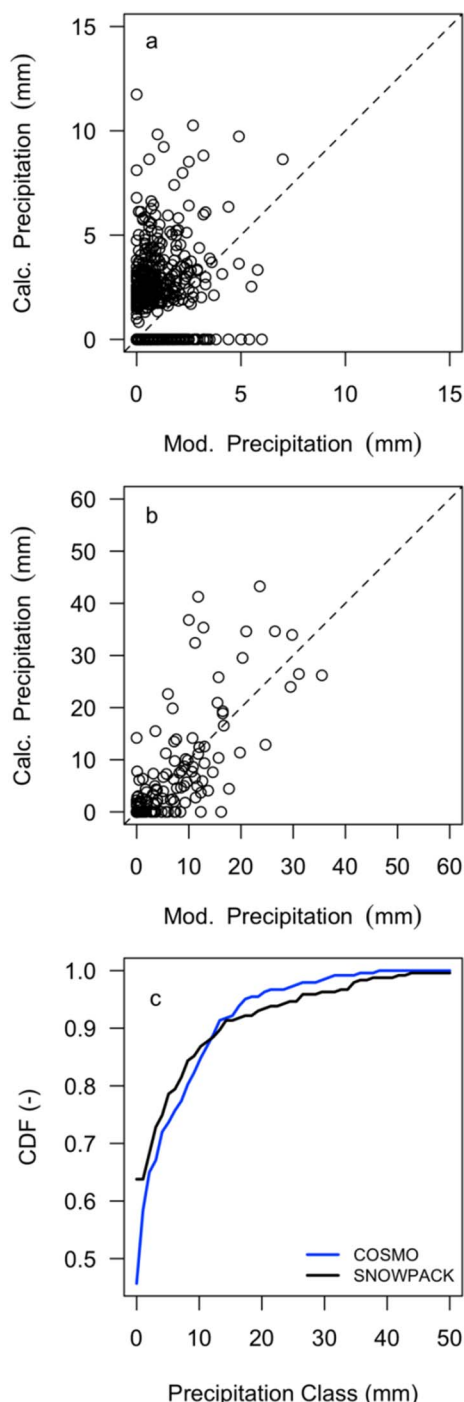


Fig. 3. Comparison of modelled (COSMO) and calculated (SNOWPACK) precipitation between October 2015 and June 2016 for the experimental site Weissfluhjoch: (a) hourly precipitation, (b) daily precipitation and (c) the cumulative density functions (CDF) for daily precipitation of COSMO (blue) and precipitations amounts derived from SNOWPACK (black). Dashed line in (a) and (b) shows the one-to-one relationship. (For interpretation of the references to colour in this figure legend, the reader is referred to the web version of this article.)

overestimated due to an overestimation of the liquid water content of the snow cover, due to enhanced melting in the simulation.

In addition to the flat field simulations we also carried out simulations for virtual south-facing slopes (Fig. 6a). Simulations for south-facing slopes tended to underestimate the LWC_{index} for all elevation bands, especially for stations above 2500 m a.s.l. This is again related to overestimating snow height on the virtual south-facing slopes using COSMO data compared to the simulation using IMIS data (not shown).

However, snow height for these slope simulations is not measured and can therefore not be verified.

To reduce the discrepancy between the forecasted LWC_{index} and the LWC_{index} obtained with station data, we used a now-cast based on SNOWPACK simulations forced with station data (IMIS) in combination with a 24-hour forecast using COSMO data. This approach removes accumulated forecasting errors, i.e. minimizes the error throughout the season, while still being able to forecast the LWC_{index} for the next day. Therefore, SNOWPACK was initiated with IMIS data as described above, but stopped daily at midnight. A SNOWPACK output file containing snow profile information was written and used to initiate the next SNOWPACK run using forecasted COSMO data as input. In other words, a daily 24-hour forecast was performed. In the following, we refer to this setup up as IMCO.

Results of the IMCO simulations for the flat site and the virtual south-facing slopes are shown in Figs. 5b and 6b, respectively. The mean absolute errors (MAE, Table 2), especially for the flat sites, were reduced. For the winter season 2015–2016, between February and May, the MAE decreased from 0.16 to 0.02 when considering all elevation bands. The largest decrease was found for stations below 2000 m a.s.l. where the MAE decreased from 0.36 to 0.04. With the IMCO setup there was almost no bias (MAE = 0.01) for stations above 2500 m a.s.l. for all years. Overall, the mean absolute errors were twice as large for the south-facing slope simulations. However, similar to the flat field simulations, the MAE also reduced significantly using the IMCO setup, e.g. for the winter season 2015–2016 for all elevation bands from 0.36 to 0.09. The greatest improvement was obtained for stations above 2500 m a.s.l. during the same winter season (0.43 to 0.08).

4.2. Wet-snow avalanche activity

Wet-snow avalanche activity (AAI) for the winter season 2015–2016 for two regions in Switzerland, i.e. Grisons and Valais, as well as the simulated LWC_{index} (IMCO, south-facing slopes) are shown in Fig. 7 for the stations located in the elevation band of 2000 to 2500 m a.s.l. (16 stations in Grisons and 14 stations in Valais).

According to Mitterer et al. (2016) a $LWC_{index} \geq 1$ indicates a critical value based on a mean volumetric liquid water content of 3% (Eq. (1)). A value of 1 was only occasionally reached in Grisons in February and March. Nevertheless, sharp increases or relatively higher values of LWC_{index} were clearly associated with increased avalanche activity. In addition, periods with no activity (early to mid-February) were associated with a low or decreasing LWC_{index} . The LWC_{index} started to increase in both regions by mid-March, reaching a value of 1 by the end of March followed by an intense wet-snow avalanche cycle lasting until the beginning of April.

We assessed the performance of different thresholds of the LWC_{index} by displaying sensitivity and specificity in a ROC diagram for each region (Fig. 8). ROC diagrams were calculated for the simulated LWC_{index} using IMIS data as well as the IMCO setup. Performance measures to predict the onset of wet-snow avalanche activity, i.e. the probability of detection (POD), the probability of non-detection (PON), the false alarm ratio (FAR) as well as the true skill statistic are compiled in Table 3. Skill scores are given for the optimal threshold values as shown in the ROC graphs (Fig. 8) as well as for the threshold values suggested by Mitterer et al. (2016).

The POD for the region of Grisons was found to be 56% for IMIS data forced SNOWPACK runs when a threshold value of 1 was used and 75% when using a threshold value of 0.33. For the region of Valais, the POD was 52% and 73% for the threshold values of 1 and 0.33, respectively. The optimal threshold value indicating wet-snow instability derived from the ROC graph for IMIS forced SNOWPACK simulations was 0.28 for Grisons and 0.24 for Valais, resulting in a POD of 82% for Grisons as well as for Valais. Different, lower, optimal threshold values were found for the LWC_{index} when using the IMCO setup, i.e. $LWC_{index} \geq 0.04$ for Grisons and Valais. The POD using the IMCO setup

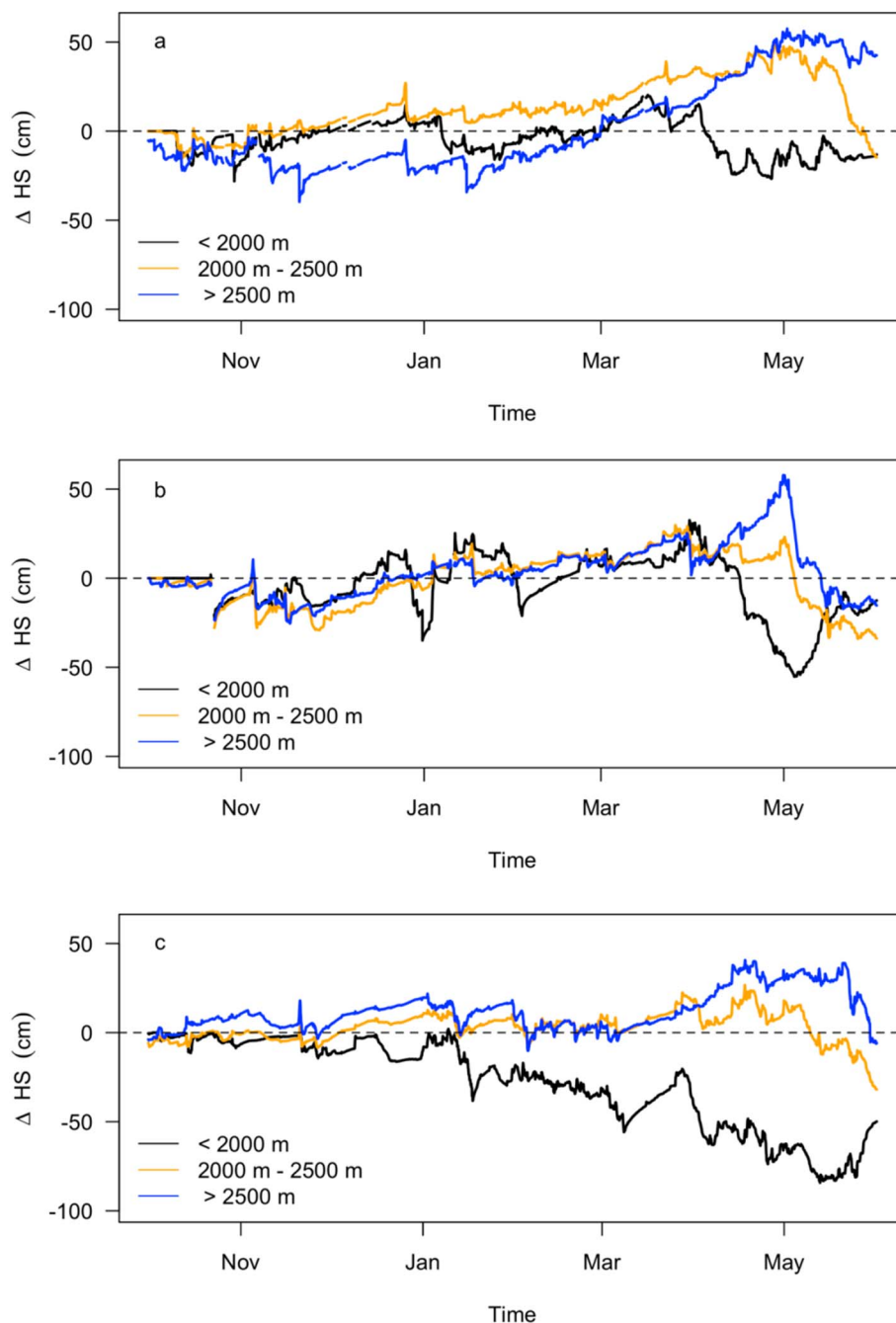


Fig. 4. Difference in snow height between SNOWPACK simulations (flat field) forced with IMIS data and those forced with COSMO data for three winter seasons: (a) 2013–2014, (b) 2014–2015 and (c) 2015–2016 between October and June. Different lines correspond to the mean difference for IMIS stations below 2000 m a.s.l. (black, $N = 17$), between 2000 m and 2500 m a.s.l. (orange, $N = 68$) as well as station above 2500 m a.s.l. (blue, $N = 28$). Dashed line is located at zero, indicating no bias. (For interpretation of the references to colour in this figure legend, the reader is referred to the web version of this article.)

with these optimal thresholds was found to be higher compared to the POD using IMIS data only, i.e. 86% for Grisons and 89% for Valais. However, for both regions and type of forcing data the FAR was high ranging between 54% and 81%. For the optimal threshold values providing the highest true skill statistic TSS ranged between 37 and 44%, and PC was between 53 and 66%. Overall, differences between the types of forcing, IMIS data vs. IMCO setup, were small.

5. Discussion

A model – not only snow cover models – can only be as good as the input data. Therefore, we compared measured meteorological parameters against their forecasted counterparts. A general cold bias was found for the forecasted COSMO data as well as a general overestimation for the incoming shortwave radiation and an underestimation for the longwave radiation (Fig. 2). No adjustments were

made for the incoming radiation provided by COSMO, therefore the overestimation of the incoming shortwave radiation might also be related to the slope of the COSMO grid cell. However, slopes of the corresponding grid cells are typically smaller than 10° and slope effects were considered rather minor.

For snow cover simulations an accurate precipitation forecast in time and space is of paramount importance. Although, the total forecasted precipitation sum for the investigated period was in good agreement with the estimated (SNOWPACK) precipitation amounts, COSMO tends to be too wet especially for smaller precipitation events (Fig. 3). The accuracy of the precipitation amounts estimated by SNOWPACK remains unknown since it strongly relies on a correct estimation of the new snow density. However, measuring winter precipitation in complex alpine terrain is very challenging (e.g., Helbig and van Herwijnen, 2017) and we assume the error to be less compared to standard methods such as rain gauges (Egli et al., 2009), since the IMIS

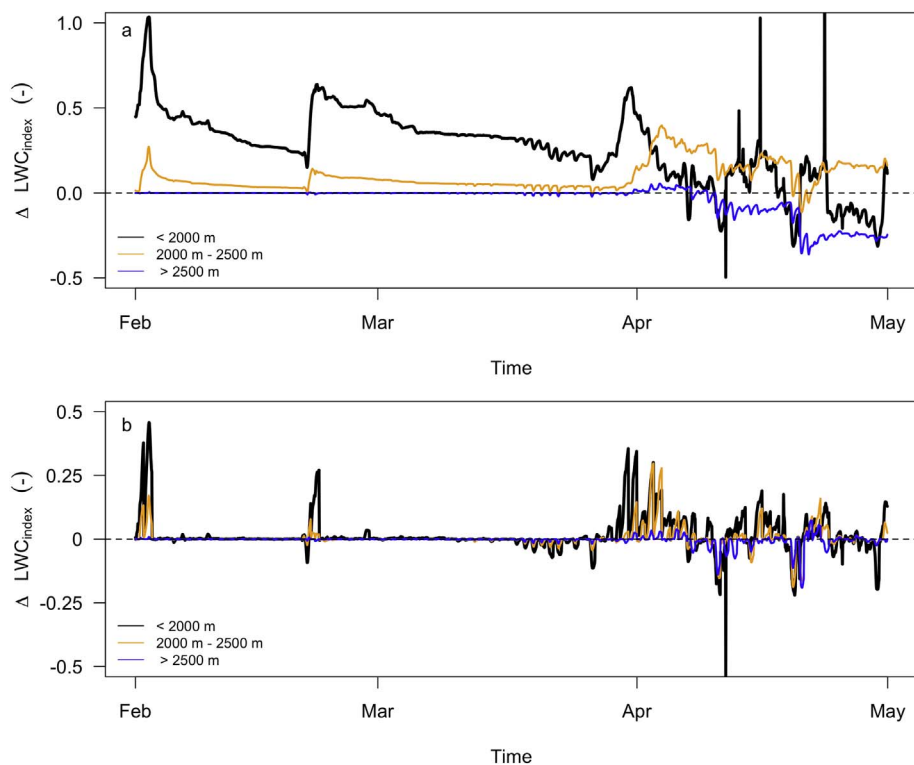


Fig. 5. Difference in LWC_{index} between SNOWPACK simulations (flat field) forced with IMIS data and (a) simulations forced with COSMO data, and (b) simulations using COSMO data in combination with SNOWPACK simulations forced with IMIS data (IMCO) for the winter season 2015–2016 between February and May. Colour-coding for elevation bands as in Fig. 4.

stations typically are not located in wind-exposed areas. However, an in-depth analysis of COSMO forecasted precipitation amounts at all locations of the IMIS network is still required.

The horizontal resolution of NWP models has significantly increased during the last years. In principal, higher horizontal resolution should allow one to forecast small-scale weather events such as convective precipitation or local wind systems. Indeed so-called convection permitting models (i.e., operational models with a resolution on the order

of 1 km) show considerably improved skill scores when compared to their coarse-resolution counterparts (e.g., Weusthoff et al., 2010). However, the physical formulations especially for turbulence and radiation, of currently available NWP models have been developed based on knowledge from flat and idealized terrain (Rotach and Zardi, 2007). Therefore, model output statistics (MOS) or bias corrections are often applied to the direct model output to correct the shortcomings of the model introduced by the model physics and underlying terrain. Future

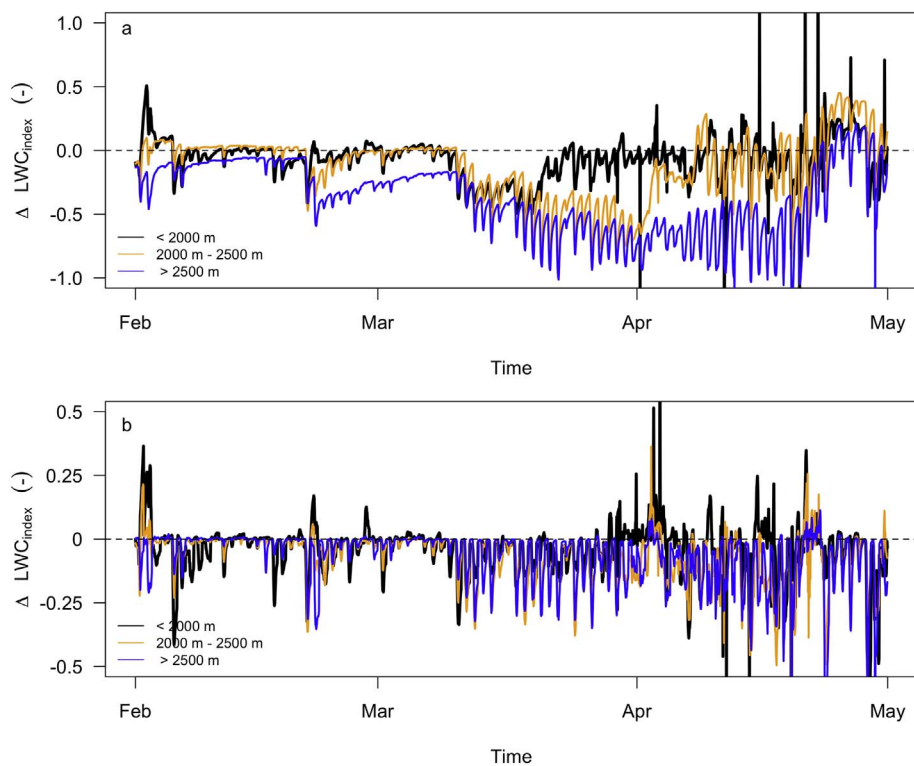


Fig. 6. Difference in LWC_{index} between SNOWPACK simulations for virtual south-facing slopes forced with IMIS data and (a) simulations forced with COSMO data, and (b) simulations using COSMO data in combination with SNOWPACK simulations forced with IMIS data (IMCO) for the winter season 2015–2016 between February and May. Colour-coding for elevation bands as described in Fig. 4.

Table 2

Mean absolute errors (MAE) of the LWC_{index} for SNOWPACK (flat and south-facing slopes) forced with COSMO as well as using the IMCO setup (a combination of IMIS and forecasted COSMO data). MAE are calculated with respect to SNOWPACK runs forced with IMIS data and given for the three winter seasons between October 2013 and June 2016 either for all IMIS stations (all) or separately for the three elevations bands.

Flat								
Season	COSMO				IMCO			
	All	< 2000 m	2000 m–2500 m	> 2500 m	All	< 2000 m	2000 m–2500 m	> 2500 m
2013–2014	0.16	0.21	0.17	0.11	0.03	0.05	0.03	0.01
2014–2015	0.10	0.18	0.08	0.10	0.02	0.03	0.02	0.01
2015–2016	0.16	0.36	0.14	0.05	0.02	0.04	0.02	0.01
South								
Season	All	< 2000 m	2000 m–2500 m	> 2500 m	All	< 2000 m	2000 m–2500 m	> 2500 m
2013–2014	0.35	0.44	0.30	0.41	0.10	0.13	0.09	0.09
2014–2015	0.35	0.38	0.35	0.36	0.09	0.12	0.09	0.08
2015–2016	0.36	0.31	0.34	0.43	0.09	0.09	0.10	0.08

improvement will therefore have to include bias corrections for relevant meteorological parameters such as air temperature, precipitation and radiation as well as improved sub-grid scale parameterization – especially for radiation and snow redistribution (Helbig and Löwe, 2012; Helbig and van Herwijnen, 2017).

When running SNOWPACK with forecasted NWP data, it is strongly advised to use the forecasted precipitation amounts, because NWP models often use simplified parameterizations for the snow cover, especially for the snow height. COSMO tends to be too wet for smaller but more frequent precipitations events (Fig. 3c) resulting – also in combination with the cold bias – in too much snow and hence an overestimation of the simulated snow height especially during the spring season (Fig. 4). Precipitation processes triggered or modified by orography are of course most challenging – even if considerable progress has been made in recent years (Richard et al., 2007). Thus, reliable point forecasts from high-resolution NWP in complex terrain – although by far the best we can obtain and more representative than a point observation – still remain a great challenge.

Bias corrections or downscaling for the NWP forcing data are required if SNOWPACK has to be run only with NWP data, e.g. in data sparse areas. Without such corrections best results were only achieved when using SNOWPACK runs forced by automated weather station data for initiation. This is especially true for the prediction of the volumetric liquid water content of the entire snow cover since the calculation of the LWC_{index} is very sensitive to the simulated snow height (Figs. 5 and 6).

High quality avalanche observations especially during the start and the end of winter season are rare (e.g. van Herwijnen et al., 2016). Therefore, the quantitative validation of the LWC_{index} on the regional and local scale (Gobiet et al., 2016) is not straightforward. Avalanche occurrence data may be inconsistent and/or incomplete (e.g., Schweizer et al., 2003). We focussed on the elevation band between 2000 and 2500 m a.s.l. where the majority of avalanches released. For the two regions of the Swiss Alps (Grisons and Valais) fair agreement between the forecasted LWC_{index} and the observed wet-snow avalanche activity was found (Fig. 7). However, major cycles of wet-snow

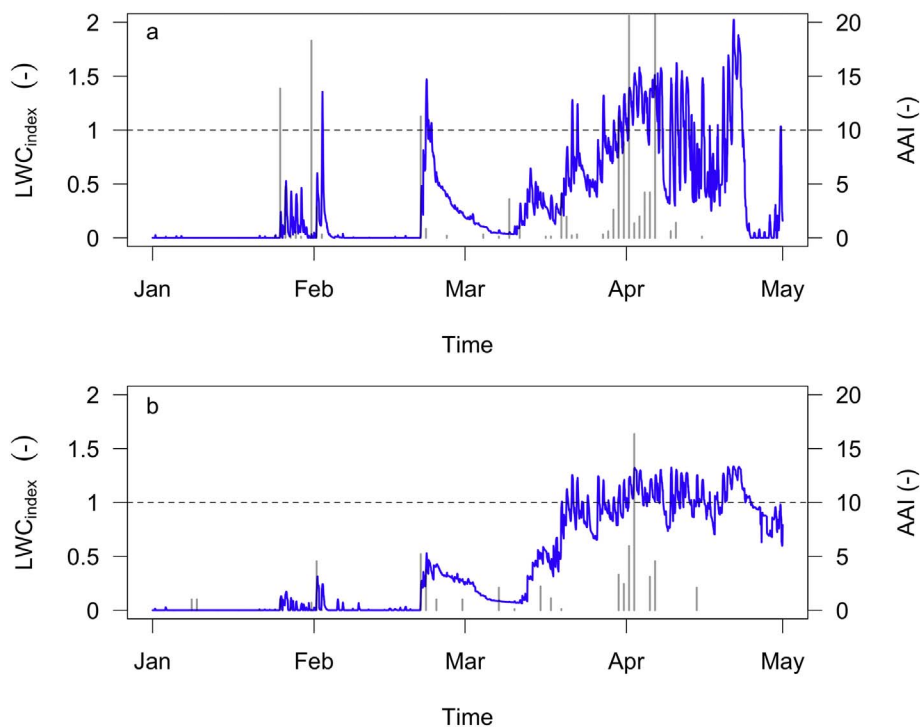


Fig. 7. Median LWC_{index} simulated with the IMCO setup (south-facing slopes, winter season 2015–2016) for the location of IMIS stations in (a) Grisons and (b) Valais for stations between 2000 m and 2500 m a.s.l. (Grisons, $N = 16$; Valais, $N = 14$). Vertical bars indicate the daily avalanche activity index (AAI) for the corresponding region. Horizontal dashed line corresponds to an LWC_{index} of 1.

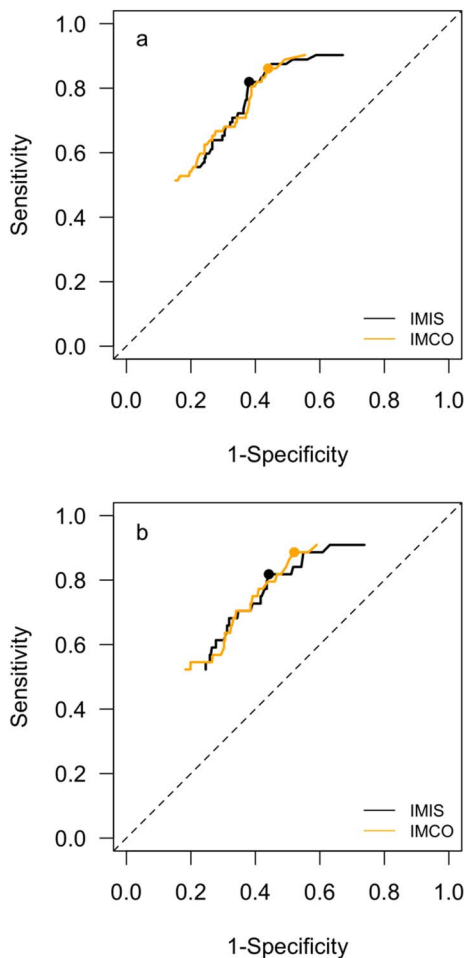


Fig. 8. Receiver operator characteristics (ROC) graph for (a) Grisons and (b) Valais. Shown are ROC's for the simulated LWC_{index} using IMIS data (black) and the IMCO setup (orange); full circles indicate the corresponding optimal threshold values (LWC_{index} , Table 3) where the true skill statistic (TSS) was maximal. (For interpretation of the references to colour in this figure legend, the reader is referred to the web version of this article.)

Table 3

Performance measures for detecting the onset of wet-snow avalanche activity using only IMIS data as input to force SNOWPACK (IMIS) as well as using the IMCO setup (a combination of IMIS and forecasted COSMO data) for the two regions of Grisons and Valais. Given are the probability of detection (POD), the probability of non-events (PON), the false alarm ratio (FAR) as well as the true skill statistic (TSS). The first two rows show the performance measures using the optimal threshold values of the LWC_{index} derived by the ROC graphs in Fig. 8. The remaining four rows show the performance measures for the threshold values suggested by Mitterer et al. (2016), i.e. $LWC_{index} \geq 0.33$ and $LWC_{index} \geq 1$, respectively.

Input	Grisons				Valais					
	Threshold				Threshold					
	LWC_{index}	POD	PON	FAR	TSS	LWC_{index}	POD	PON	FAR	TSS
–	(%)	(%)	(%)	(%)	–	(%)	(%)	(%)	(%)	
IMIS	≥ 0.28	82	62	65	44	≥ 0.24	82	56	80	38
IMCO	≥ 0.04	86	56	67	42	≥ 0.04	89	48	81	37
IMIS	≥ 0.33	75	63	66	38	≥ 0.33	73	59	80	32
IMCO	≥ 0.33	71	66	66	37	≥ 0.33	70	66	78	36
IMIS	≥ 1	56	78	61	34	≥ 1	52	75	77	28
IMCO	≥ 1	51	85	54	36	≥ 1	52	82	72	34

avalanche activity, e.g. 31 January 2016 (Fig. 7a), were not captured. The event on 31 January 2016 (Fig. 7a) was a confirmed rain-on-snow event, which was not detected by neither the simulation with IMIS data nor by the IMCO setup. SNOWPACK uses a static threshold of $+1.2\text{ }^\circ\text{C}$ to distinguish between precipitation falling as snow (smaller than threshold) or rain (larger than threshold). Rain-on-snow events will drastically increase the liquid water content of the snow cover and hence increase the LWC_{index} . Using additional NWP data, e.g. air temperature from vertical levels of a NWP model or the predicted snow line, might further improve the simulations.

Mitterer et al. (2016) suggested two critical thresholds for the onset of wet-snow avalanche activity depending on the scale of the study area and the flow regime, namely $LWC_{index} \geq 1$ and $LWC_{index} \geq 0.33$. Optimal threshold values (Table 3), based on our data set, were found to be lower than the threshold of 1 suggested by Mitterer et al. (2013) who also predicted the onset of wet-snow avalanche activity at the regional scale. The lower values we found might be related to an overestimation of simulated snow height compared to the actual snow height in starting zones (e.g., Mitterer et al., 2011). If the snow height is too high, the LWC_{index} becomes too low.

The POD values tended to be rather low using a threshold of ≥ 1 . We selected the optimal thresholds based on maximizing TSS that considers both the hits and the false alarms (Table 1, Eq. (5)). Of course higher POD values can be achieved with lower thresholds such as 0.33, but on the expense of a higher number of false alarms. It may depend on the forecast problem at hand, in particular on the cost of an incorrect forecast, whether to give more weight to high POD or to low FAR. Any skill score is inherently only a scalar measure of forecast performance. In fact, three measures are required to fully describe the verification data summarized in a 2×2 contingency table, since its dimensionality is 3 (Wilks, 2011; p. 308).

After a period of high wet-snow avalanche activity the LWC_{index} typically stays high with strong diurnal changes (Fig. 7a), but without significant avalanche activity. This behaviour partly explains the high values of the false alarm ratio (FAR). The primary cause for the extended period of high values of the LWC_{index} is related to how the bucket water transport scheme within SNOWPACK handles the movement of water. Based on snow density, the water transport scheme allows for a residual amount of water to be kept within the snow cover. In other words, this is the amount of water that does not drain and/or refreezes and hence is kept within the snowpack until the snowpack melts out completely. This residual volumetric liquid water content is normally around 3%, which corresponds to a LWC_{index} of around 1. Reducing the FAR would require refining the classification by, e.g., neglecting large values of the LWC_{index} after a confirmed avalanche cycle and before the next snowfall.

In addition, the bucket water transport scheme in SNOWPACK is based on simple assumptions and certainly oversimplifies the complex flow behaviour of water in snow. There are more complex approaches implemented in SNOWPACK (e.g., Wever et al., 2015; Wever et al., 2016b), but these are currently not fully available as operational supporting tools. Future work will include simulations using these more complex water transport schemes based on Richards' Equation and/or a parameterisation of preferential flow paths, which in turn should improve the simulation of liquid water content and hence the prediction of the LWC_{index} .

The COSMO data were not bias corrected – or statistically down-scaled – except for adjusting the forecasted air temperature to the elevation difference between COSMO grid point and station elevation. A bias correction should further enhance the performance of the IMCO model chain in terms of timing of wet-snow avalanche activity.

6. Conclusions

To forecast wet-snow avalanche activity, we forced the snow cover model SNOWPACK with input data from a network of automated

weather stations (AWS; IMIS) as well as data from the numerical weather prediction model COSMO with a horizontal resolution of 1 km. The onset of wet-snow avalanche activity was estimated by simulating a recently developed index based on the average volumetric liquid water content of the entire snow cover (LWC_{index}).

As previously shown, the LWC_{index} calculated with SNOWPACK forced with data from automated weather stations, can indicate the onset of wet-snow avalanche activity. However, up to now only a now-cast was possible using AWS data. Although forcing SNOWPACK with forecasted data from COSMO shows promising potential, not only for wet-snow avalanche activity, corrections of input parameters for the evolution of the snow cover are still required. Using SNOWPACK simulations forced with data from automated weather stations as initial state and subsequently adding forecasted data removes the accumulated error. By using a combination of measured and forecasted data the LWC_{index} predicted the onset of wet-snow avalanche activity reasonably well with very similar accuracy as forced with IMIS data (now-cast). While using optimal thresholds for the LWC_{index} , the probability of detection was between 86% and 88% for three winters between 2013 and 2016 and for two different climate regions in Switzerland.

Here we focused on forecasting wet-snow instability. In general, forcing state-of-the-art snow cover models with high-resolution numerical weather prediction models allows combining snow cover, stability and weather information, i.e. the key ingredients for avalanche forecasting. Therefore, a coupled snow cover and NWP model represents a powerful tool for avalanche warning services.

Acknowledgements

COSMO data as well as computational resources were kindly provided by the Federal Office of Meteorology and Climatology MeteoSwiss. For general support and discussions about the COSMO data we would like to thank Reto Stauffer (University of Innsbruck) and André Walser (MeteoSwiss). The project was partly funded by the Austrian Science Fund (FWF): Project No.: M01521; Project Name: SAINT.

References

- Baggi, S., Schweizer, J., 2009. Characteristics of wet snow avalanche activity: 20 years of observations from a high alpine valley (Dischma, Switzerland). *Nat. Hazards* 50 (1), 97–108.
- Bartelt, P., Lehning, M., 2002. A physical SNOWPACK model for the Swiss avalanche warning; part I: numerical model. *Cold Reg. Sci. Technol.* 35 (3), 123–145.
- Bellaire, S., Jamieson, B., 2013a. Forecasting the formation of critical snow layers using a coupled snow cover and weather model. *Cold Reg. Sci. Technol.* 94, 37–44.
- Bellaire, S., Jamieson, B., 2013b. On estimating avalanche danger from simulated snow profiles. In: Naaim-Bouvet, F., Durand, Y., Lambert, R. (Eds.), *Proceedings ISSW 2013. International Snow Science Workshop, Grenoble, France, 7–11 October*. Vol. 2013. ANENA, IRSTEA, Météo-France, Grenoble, France, pp. 154–161.
- Bellaire, S., Jamieson, J.B., Fierz, C., 2011. Forcing the snow-cover model SNOWPACK with forecasted weather data. *Cryosphere* 5 (4), 1115–1125.
- Brun, E., 1989. Investigation on wet-snow metamorphism in respect of liquid-water content. *Ann. Glaciol.* 13, 22–26.
- Brun, E., David, P., Sudul, M., Brunot, G., 1992. A numerical model to simulate snow-cover stratigraphy for operational avalanche forecasting. *J. Glaciol.* 38 (128), 13–22.
- Denoth, A., 1980. The pendular-funicular liquid transition in snow. *J. Glaciol.* 25 (91), 93–97.
- Doms, G., Schättler, U., 2002. A description of the nonhydrostatic regional model LM. In: Part I: Dynamics and Numerics. Deutscher Wetterdienst, Offenbach (Available at: <http://www.cosmo-model.org>).
- Durand, Y., Giraud, G., Brun, E., Mérindol, L., Martin, E., 1999. A computer-based system simulating snowpack structures as a tool for regional avalanche forecasting. *J. Glaciol.* 45 (151), 469–484.
- Egli, L., Jonas, T., Meister, R., 2009. Comparison of different automatic methods for estimating snow water equivalent. *Cold Reg. Sci. Technol.* 57 (2–3), 107–115.
- Gobiet, A., Mitterer, C., Jöbstl, L., Steinkogler, W., Rieder, H., Olefs, M., Studerregger, A., Monti, F., Bellaire, S., 2016. Operational forecasting of wet snow avalanche activity: a case study for the Eastern European Alps. In: *Proceedings ISSW 2016. International Snow Science Workshop, Breckenridge CO, U.S.A., 3–7 October 2016*.
- Helbig, N., Löwe, H., 2012. Shortwave radiation parameterization scheme for subgrid topography. *J. Geophys. Res.* 117 (D3), D03112.
- Helbig, N., van Herwijnen, A., 2017. Subgrid parameterization for snow depth over mountainous terrain from flat field snow depth. *Water Resour. Res.* 53, 1444–1456.
- Helbig, N., Löwe, H., Mayer, B., Lehning, M., 2010. Explicit validation of a surface shortwave radiation balance model over snow-covered complex terrain. *J. Geophys. Res.* 115, D18113.
- Helbig, N., van Herwijnen, A., Jonas, T., 2015. Forecasting wet-snow avalanche probability in mountainous terrain. *Cold Reg. Sci. Technol.* 120, 219–226.
- van Herwijnen, A., Heck, M., Schweizer, J., 2016. Forecasting snow avalanches by using avalanche activity data obtained through seismic monitoring. *Cold Reg. Sci. Technol.* 132, 68–80.
- Lafaysse, M., Morin, S., Coléou, C., Vernay, M., Serça, D., Besson, F., Willemet, J.M., Giraud, G., Durand, Y., 2013. Toward a new chain of models for avalanche hazard forecasting in French mountain ranges, including low altitude mountains. In: Naaim-Bouvet, F., Durand, Y., Lambert, R. (Eds.), *Proceedings ISSW 2013. International Snow Science Workshop, Grenoble, France, 7–11 October*. Vol. 2013. ANENA, IRSTEA, Météo-France, Grenoble, France, pp. 162–166.
- Lehning, M., Bartelt, P., Brown, R.L., Russi, T., Stöckli, U., Zimmerli, M., 1999. Snowpack model calculations for avalanche warning based upon a new network of weather and snow stations. *Cold Reg. Sci. Technol.* 30 (1–3), 145–157.
- Lehning, M., Bartelt, P., Brown, R.L., Fierz, C., 2002a. A physical SNOWPACK model for the Swiss avalanche warning; part III: meteorological forcing, thin layer formation and evaluation. *Cold Reg. Sci. Technol.* 35 (3), 169–184.
- Lehning, M., Bartelt, P., Brown, R.L., Fierz, C., Satyawali, P.K., 2002b. A physical SNOWPACK model for the Swiss avalanche warning; part II. Snow microstructure. *Cold Reg. Sci. Technol.* 35 (3), 147–167.
- McClung, D.M., Schaerer, P., 2006. *The Avalanche Handbook*. The Mountaineers Books, Seattle WA, U.S.A. (342 pp.).
- Mitterer, C., Schweizer, J., 2013. Analysis of the snow-atmosphere energy balance during wet-snow instabilities and implications for avalanche prediction. *Cryosphere* 7 (1), 205–216.
- Mitterer, C., Hirashima, H., Schweizer, J., 2011. Wet-snow instabilities: comparison of measured and modelled liquid water content and snow stratigraphy. *Ann. Glaciol.* 52 (58), 201–208.
- Mitterer, C., Techel, F., Fierz, C., Schweizer, J., 2013. An operational supporting tool for assessing wet-snow avalanche danger. In: Naaim-Bouvet, F., Durand, Y., Lambert, R. (Eds.), *Proceedings ISSW 2013. International Snow Science Workshop, Grenoble, France, 7–11 October*. Vol. 2013. ANENA, IRSTEA, Météo-France, Grenoble, France, pp. 334–338.
- Mitterer, C., Heilig, A., Schmid, L., van Herwijnen, A., Eisen, O., Schweizer, J., 2016. Comparison of measured and modelled snow cover liquid water content to improve local wet-snow avalanche prediction. In: Greene, E. (Ed.), *Proceedings ISSW 2016. International Snow Science Workshop, Breckenridge CO, U.S.A., 3–7 October 2016*, pp. 125–131.
- Peitzsch, E.H., Hendriks, J., Fagre, D.B., Reardon, B., 2012. Examining spring wet slab and glide avalanche occurrence along the Going-to-the-Sun Road corridor, Glacier National Park, Montana, USA. *Cold Reg. Sci. Technol.* 78, 73–81.
- Quéno, L., Vionnet, V., Dombrowski-Etchevers, I., Lafaysse, M., Dumont, M., Karbou, F., 2016. Snowpack modelling in the Pyrenees driven by kilometeric-resolution meteorological forecasts. *Cryosphere* 10 (4), 1571–1589.
- Richard, E., Buzzi, A., Zängl, G., 2007. Quantitative precipitation forecasting in the Alps: the advances achieved by the Mesoscale Alpine Programme. *Q. J. R. Meteorol. Soc.* 133 (625), 831–846.
- Romig, J.M., Custer, S.G., Birkeland, K.W., Locke, W.W., 2005. March wet avalanche prediction at Bridger Bowl Ski Area, Montana. In: Elder, K. (Ed.), *Proceedings ISSW 2004. International Snow Science Workshop, Jackson Hole WY, U.S.A., 19–24 September 2004*, pp. 598–607.
- Rotach, M.W., Zardi, D., 2007. On the boundary-layer structure over highly complex terrain: Key findings from MAP. *Q. J. R. Meteorol. Soc.* 133 (625), 937–948.
- Schirmer, M., Jamieson, B., 2015. Verification of analysed and forecasted winter precipitation in complex terrain. *Cryosphere* 9 (2), 587–601.
- Schmid, L., Heilig, A., Mitterer, C., Schweizer, J., Maurer, H., Okorn, R., Eisen, O., 2014. Continuous snowpack monitoring using upward-looking ground-penetrating radar technology. *J. Glaciol.* 60 (221), 509–525.
- Schmucki, E., Marty, C., Fierz, C., Lehning, M., 2014. Evaluation of modelled snow depth and snow water equivalent at three contrasting sites in Switzerland using SNOWPACK simulations driven by different meteorological data input. *Cold Reg. Sci. Technol.* 99, 27–37.
- Schneebeil, M., 2004. Mechanisms in wet snow avalanche release. In: *Proceedings ISSMA-2004, International Symposium on Snow Monitoring and Avalanches. Snow and Avalanche Study Establishment, India, Manali, India, 12–16 April 2004*, pp. 75–77.
- Schweizer, J., Jamieson, J.B., 2007. A threshold sum approach to stability evaluation of manual snow profiles. *Cold Reg. Sci. Technol.* 47 (1–2), 50–59.
- Schweizer, J., Kronholm, K., Wiesinger, T., 2003. Verification of regional snowpack stability and avalanche danger. *Cold Reg. Sci. Technol.* 37 (3), 277–288.
- Schweizer, J., Mitterer, C., Stoffel, L., 2009. On forecasting large and infrequent snow avalanches. *Cold Reg. Sci. Technol.* 59 (2–3), 234–241.
- Techel, F., Pielmeier, C., 2009. Wet snow diurnal evolution and stability assessment. In: Schweizer, J., van Herwijnen, A. (Eds.), *International Snow Science Workshop ISSW, Davos, Switzerland, 27 September–2 October 2009*. Swiss Federal Institute for Forest, Snow and Landscape Research WSL, pp. 256–261.
- Trautman, S., Lutz, E.R., Birkeland, K.W., Custer, S., 2006. Relating wet loose snow avalanching to surficial shear strength. In: Gleason, J.A. (Ed.), *Proceedings ISSW 2006. International Snow Science Workshop, Telluride CO, U.S.A., 1–6 October 2006*, pp. 71–78.
- Vernay, M., Lafaysse, M., Mérindol, L., Giraud, G., Morin, S., 2015. Ensemble forecasting of snowpack conditions and avalanche hazard. *Cold Reg. Sci. Technol.* 120, 251–262.
- Vionnet, V., Brun, E., Morin, S., Boone, A., Faroux, S., Le Moigne, P., Martin, E., Willemet, J.M., 2012. The detailed snowpack scheme Crocus and its implementation in SURFEX

- v7.2. *Geosci. Model Dev.* 5 (3), 773–791.
- Vionnet, V., Dombrowski-Etchevers, I., Lafaysse, M., Quéno, L., Seity, Y., Bazile, E., 2016. Numerical weather forecasts at kilometer scale in the French Alps: evaluation and application for snowpack modeling. *J. Hydrometeorol.* 17 (10), 2591–2614.
- Weusthoff, T., Ament, F., Arpagaus, M., Rotach, M.W., 2010. Assessing the benefits of convection-permitting models by neighborhood verification: examples from MAP D-PHASE. *Mon. Weather Rev.* 138 (9), 3418–3433.
- Wever, N., Schmid, L., Heilig, A., Eisen, O., Fierz, C., Lehning, M., 2015. Verification of the multi-layer SNOWPACK model with different water transport schemes. *Cryosphere* 9 (6), 2271–2293.
- Wever, N., Valero, C.V., Fierz, C., 2016a. Assessing wet snow avalanche activity using detailed physics based snowpack simulations. *Geophys. Res. Lett.* 43, 5732–5740.
- Wever, N., Würzer, S., Fierz, C., Lehning, M., 2016b. Simulating ice layer formation under the presence of preferential flow in layered snowpacks. *Cryosphere* 10 (6), 2731–2744.
- Wilks, D.S., 2011. Statistical methods in the atmospheric sciences. In: *International Geophysics Series 100* Academic Press, San Diego CA, U.S.A. (467 pp.).